

VISUALISATION OF THE BUBBLE DETACHMENT AT A DIP TUBE

*G. Janssens-Maenhout, L. Dechamp
Joint Research Centre Ispra
Via Fermi, 1, I-21020 ISPRA, Italy*

ABSTRACT

In accountancy tanks of reprocessing facilities the pneumericator known as dip tube technique is commonly used for level measurements, because the pneumericator delivers accurate measurements and the dip tubes are robust and easy in maintenance. The traditional pneumericator consists in three dip tubes of steel with a flat end and different lengths, all connected to the same air flow supply. The liquid level is measured by means of the hydrostatic head at the bubbling tip of the immersed dip tube.

The internal diameter has a major impact on the pressure build up on one hand and on the clogging of the tips on the other hand. Blockage or plugging of the dip tubes usually occurs in tanks with highly concentrated solutions. Therefore a regular check of the operation of the dip tube at very small gas flow rate is performed. Under these conditions, hereafter called slow bubbling mode the bubble formation and especially the bubble detachment gives detailed information on the status of the tip. As the dip tube starts clogging, smaller bubbles are detaching with a higher frequency. This can only be visualized by the pressure signal if the detachment frequency is low enough. For carrying out this check in slow bubbling mode the pneumericator has to be taken out of normal operation for a longer period of time. An alternative method for checking the tip's status is by recording the bubble detachment in the normal fast operation mode with an electrical conductivity signal. Both methods are evaluated in this paper.

The bubble formation and detachment have been experimentally investigated for slow and fast mode by analysing the traditional pressure signal and the alternative electrical conductivity signal, acquired with a data rate of 10kHz and in synchronisation with camera pictures. In the case of slow bubbling mode the pressure signal yields most information on the bubble detachment, whereas in the case of fast bubbling mode the electrical conductivity is to be preferred. Influence of the supplied air flow rate, of the solution's salt concentration and density and of the tip's depth have been taken into account.

1. INTRODUCTION

For safeguards reasons all nuclear material in a nuclear facility has to be accounted for and inspected by Euratom or the IAEA. A reprocessing plant treats the nuclear material in different forms (solid, liquid or vapour) and the inventory is made at well-defined key measurement points, such as the accountancy tank for the input and output solution. Each input/output accountancy tank is equipped with a pneumericator system to monitor the volume and density of the nuclear solution.

The traditional configuration of a pneumericator system at a reprocessing tank consists in three dip tubes of steel with a flat end and different lengths. The external diameter of each dip tube is typically 10mm and the internal diameter 6mm. The level dip tube is the longest one, the density dip tube ends on a well-defined probe separation distance S above the level dip tube and the reference dip tube never dips into the solution. In most cases absolute pressures at the dip tube's bubbling tip, respectively p_L , p_D and p_R are measured by three separate pressure transducers, although also the differential configuration exists where two pressure transducers measure $p_L - p_R$ and $p_L - p_D$. The density ρ_L is then derived by

$(p_L - p_D)/(gS)$, and the level l by $(p_L - p_R)/(rg)$, and the volume is derived with the measured level and temperature, utilising the calibration curve of the tank $V(l, T)$. The flat shape of the tip of the dip tube has been selected in most cases, since studies on other shapes of the dip tube's tip, such as performed by Uchikoshi (1996), did not show a clear advantage.

The air bubbling causing up and down movements of the solution in the lowest part of the dip tube can cause drying out of the thin liquid films. Hence precipitation of salts of the concentrated solution occurs and solid particles deposit on the internal wall of the dip tube. Clogging of dip tubes is partially anticipated by installation of instrument air humidifiers after the air flow meter on the air supplying line. However the status of the dip tube's tip remains to be surveyed in order to keep the pressure measurements accurate.

This paper investigates various methods for checking the tip's status by recording the bubble detachment in slow, medium

and fast operation mode. Three types of signals are utilised to experimentally invest the detachment of a bubble at the dip tube's tip.

2. BUBBLE DETACHMENT PHENOMENA

2.1 Experimental Setup

The experiments have been carried out in an open plexi-glass cylinder of 280mm internal diameter and filled up with tap water up to 450mm height. The water bath was located in an air-conditioned room at 20°C. A steel dip tube with internal diameter of 6mm and external diameter of 10mm, which was insulated by a polyethylene cover of 3mm thickness, was dipping into the water. Normal dry air was supplied to the dip tube with an air flow rate varying between 3l/hr and 15l/hr.

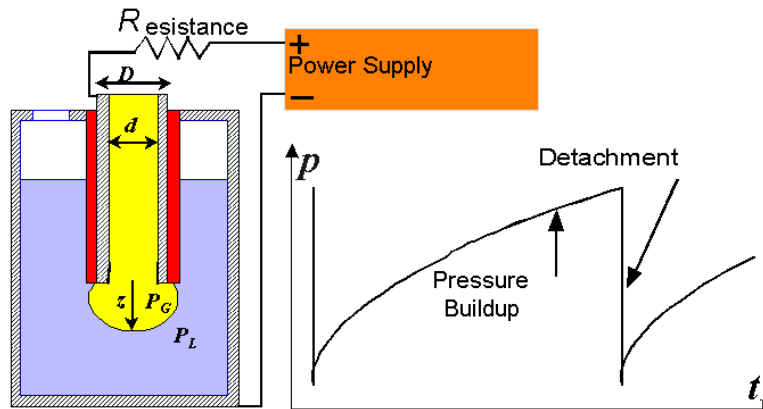


Fig. 1: Experimental Setup for bubble detachment measured by pressure and electrical conductivity signal.

An electrical circuit has been constructed with an external resistance of 1.5kΩ, as indicated by the sketch of the experimental setup in Fig. 1. The electrical conductivity of the water was estimated to be 50μS/cm. As long as the water was in contact with the inner steel tube, the voltage measured over the resistance was maximal. Once a bubble was formed with a diameter exceeding 10mm, the voltage dropped down dramatically.

The pressure on the dip tube was measured by a small pressure transducer, based on the principle of strain changes in a Wheatstone bridge configuration. This pressure transducer was operated with a data acquisition rate of 10 kHz and an accuracy of 2Pa. The performance of the pressure transducer, especially the

stability and reproducibility of the measurements, was checked against the well performing Digital Pressure Module¹, which measures the pressure based on the vibrating cylinder principle.

The voltage related to the electrical conductivity was visualised by an oscilloscope² with an acquisition rate up to 10kHz and a relative accuracy of 1%. The detachment of the bubble could be followed accurately by the very steep slope of the electrical signal without delay. However if the bubble was detaching

¹ The Digital Pressure Module is manufactured by the Weston Aerospace Co.

² The Gage Scope System of the Tektronix Technology Co. was utilised as software for controlling the oscilloscope and data-acquisition boards.

before reaching the size with mean diameter of 10mm, the bubble was not detected. The internal PC clock has been used to allocate the time for both measurements and to synchronise the electrical signal with the pressure signal.

2.2 Modelling of the Bubble Detachment

The pressure behaviour allows to follow the bubble formation and detachment at the tip of the dip tube. The bubble formation is traditionally visualized by a smooth pressure increase, whereas the bubble detachment corresponds to an abrupt pressure drop (see Fig. 1). This yields the typical pressure signal of Fig. 2, an example recorded with the pressure transducer.

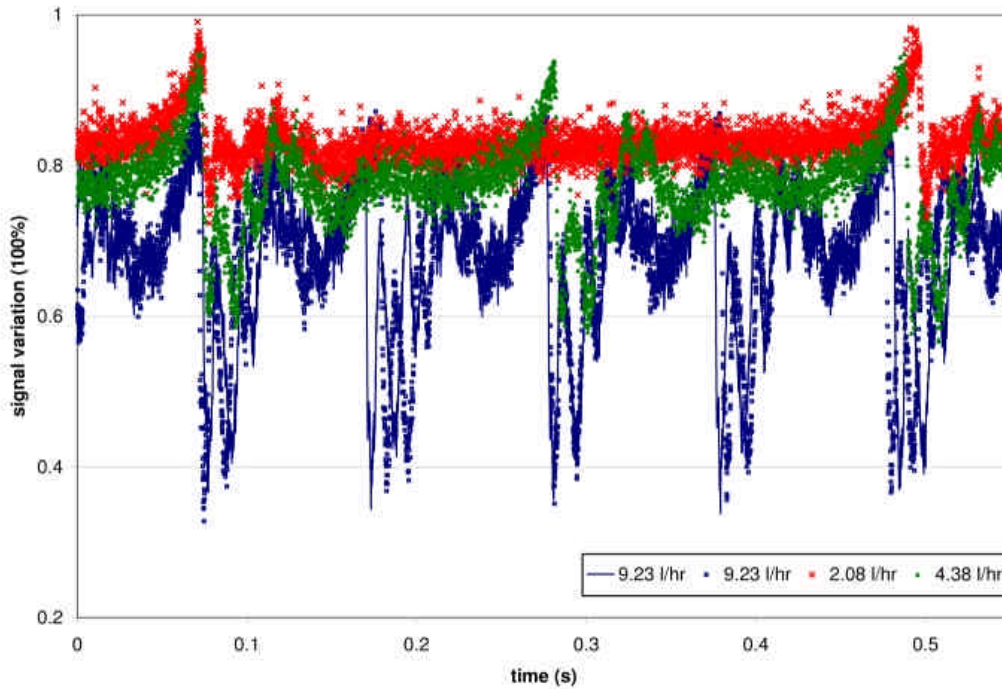


Fig. 2: Typical signal for the pressure recorded at the tip of a bubbling dip tube, for different gas flow rates.

Both the amplitude as well as the frequency of the periodical pressure signal depend on the gas flow rate and on the maximum bubble volume. The influencing parameters of the gas-liquid system are the liquid properties with density ρ_L , with dynamic viscosity μ and with surface tension σ , the dip tube's geometry with internal diameter d and external diameter D , and with the supplied volumetric gas flow rate Q . According to Georgescu (2001) the maximum bubble volume V , which is reached at the moment of detachment can be well derived with the mean detachment bubble diameter or so-called Sauter diameter S_B in the relationship of Tate (1864):

$$(\rho_L - \rho_G)gV = \rho S_B \sigma \quad (1)$$

if a quasi-static detachment occurs. This equation expresses that under quasi-static conditions, which are only fulfilled in the limited case of extreme slow bubbling mode, the Archimedes force and the

surface tension force are in balance at the point of detachment.

With the coordinates as given in Fig. 1 the bubble at its maximum size can be assumed to be an ellipsoid, which is symmetrically around the vertical axis with width D_B and with height z . With the balance of Eq. 1 the height or distance z below the dip tube's tip is determined by

$$z D_B^2 (\rho_L - \rho_G) g = 6 S_B \sigma \quad (2).$$

The height z can be measured by the maximum pressure variation. If the maximum bubble width D_B is assumed to reach the outer diameter of the dip tube D without departing it, then the Sauter diameter S_B can be estimated with Eq. 2 and the volume V can be calculated with Eq. 1. The derived maximum bubble volumes for the different pressure measurements are in agreement with the results of Platzer et al. (1985). The quasi-static assumptions are acceptable.

Of course the bubble detachment is a dynamic process, and in particular an instability problem. The form of the bubble can be calculated by considering the velocity potential of an irrotational liquid flow around the expanding bubble. Since the flow is symmetric around the dip tube's axis, we concentrate on the normal component of the velocity potential $\mathbf{j} = \partial v_n / \partial n$. The gas velocity at the tip of the dip tube is determined by:

$$u = 4Q / (\pi d^2) \quad (3).$$

After introducing the following scaling:

$$p^* = \frac{p - \mathbf{r}_L g l}{2\mathbf{s}/d}, \quad v_n^* = \frac{v_n}{u}, \quad (4)$$

$$t^* = \frac{2u t}{d}, \quad z^* = \frac{z}{d/2}$$

and applying the Bernoulli equation for the dimensionless normal component of the velocity potential \mathbf{j}^* yields for the dimensionless Sauter diameter $S_B^* = S_B/d$ the following four terms:

$$\frac{2}{S_B^*} = p^* + Eo z^* + \frac{1}{We} \left(\frac{\partial \mathbf{j}^*}{\partial t^*} + \frac{1}{2} |\nabla^* \mathbf{j}^*|^2 \right) + 2Ca \frac{\partial^2 \mathbf{j}^*}{\partial n^{*2}} \quad (5).$$

The first term on the right hand side of Eq. 5 describes the ratio of the inertial pressure force to the surface tension force, the second term indicates the gravity importance against the surface tension force with the Eötvös Number, defined as $Eo = \mathbf{r}_L g d^2 / (2\mathbf{s})$. The third term addresses the instability problem with the Weber Number given by $We = \mathbf{r}_L u^2 d / \mathbf{s}$ and the last term describes the ratio of the viscosity forces to the surface tension forces with the Capillary Number given by $Ca = \mu / \mathbf{s}$. For the investigated case of an air-water system and the typical gas flow rate varying from 3l/hr to 15 l/hr through a dip tube with internal diameter of 6mm the order of magnitude for the Eo , We and Ca numbers is given in Table 1.

d (mm)	Q (l/hr)	Eo	We	Ca
6	3	2.26	0.07	0.00040
6	9	2.26	0.64	0.00121
6	15	2.26	1.78	0.00202
4	3	1.00	0.24	0.00090
4	9	1.00	2.16	0.00273
4	15	1.00	6.01	0.00454

Table 1: Eötvös, Weber and Capillary number for an air bubbling dip tube in water with diameter d and gas flow rate Q .

Under the conditions considered in this paper, the Capillary Number is so small that the last term in Eq. 5 can be neglected and the problem can be treated in the inviscid limit.

As already noticed by Rayleigh (1899) sufficient time must be allowed for the formation of the bubbles. If the time is not sufficiently long, instead of bubble by bubble release, one observes the formation of a bubble jet. The transition from single bubbling to jetting appears to occur at the critical Weber number We_c . This has been investigated for liquid-liquid systems by Cliff (1978) and for liquid-gas

(droplet) systems by Clane (1999). The instability problem at the tip of a hanging tube for the droplet system differs from the one for the bubble system because the Rayleigh-Taylor instability and the therewith related necking is absent in the latter case.

However concerning the transition from bubbling to jetting and back to bubbling a similar hysteresis effect was observed as in the case of transition from dropping to jetting and back to dropping. After a bubble is released from the tube, the edge of the remaining liquid after the pinching

d (mm)	D (mm)	We	We_c
4	8	2.16	7
6	10	0.64	5
6	12	0.64	8

Table 2: Weber number and critical Weber number for a bubbling dip tube in water with internal diameter d , external diameter D and an air flow rate of 9 l/hr.

off begins to recede under the strong pull of surface tension forces. For the bubble system a longer period of interface oscillation is observed than for the droplet system. The dynamics of recession can however in both cases be described with the extension model of Taylor (1959) for the receding motion of a rim. Based on this model Clane derived the critical Weber Number as a function of the classical Eötvös number, built with the internal diameter and the modified Eötvös number built with the external diameter of the dip tube D . The order of magnitude of the critical Weber number for the above mentioned case has been given in Table 2. The normal operation conditions lead to a Weber number, which is smaller than the

critical Weber number. Therefore no jetting is further considered here.

3. VISUALISATION OF THE BUBBLE DETACHMENT

With a high speed camera a sequence of bubble formations and detachments has been analysed for slow bubbling mode and the recorded pressure signal for one bubble has been interpreted. In Fig. 3 an example is given of the pressure recorded with 10 kHz for one bubble, from formation till detachment, as shown in the camera pictures, taken with a rate of 30 frames/s.

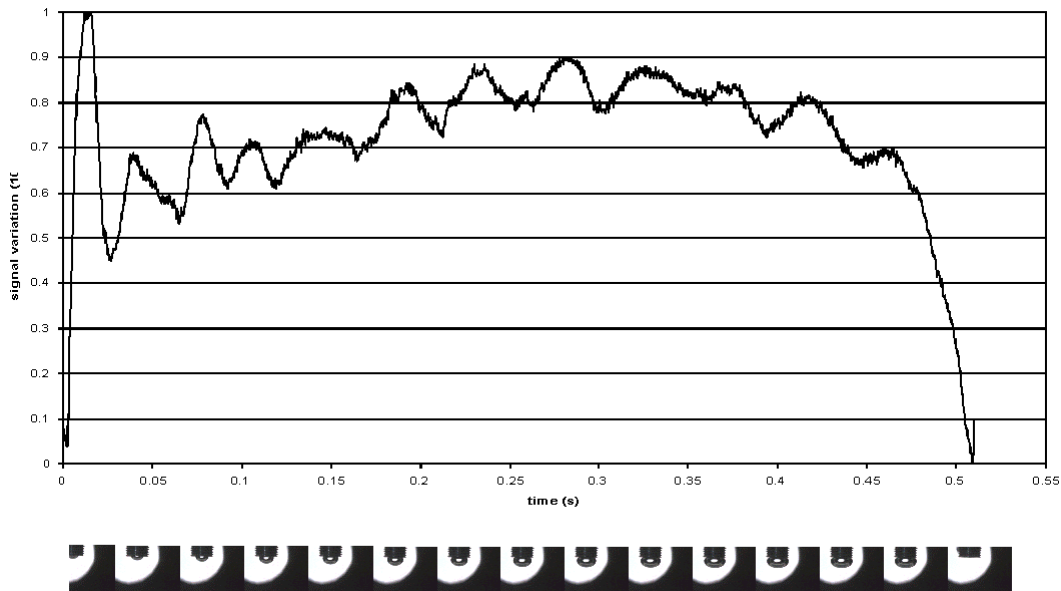


Fig. 3: Visualisation of a bubble formation sequence until detachment with camera.

inside and outside at the exit or tip of the dip tube. Then the dynamic bubble growth is gradually performed by a steadily increasing pressure build-up with small dynamic steps, which may correspond to the bubble oscillation. The pressure increase corresponds to the expansion of the gas/liquid-interface downwards the dip tube's tip. After the maximum height z (for the given air flow rate) is reached, the bubble starts enlarging (with increasing D_B), increasing its volume V without enhancing the mean internal pressure. In the contrary the bubble contracts in the vertical direction slightly to expand more in the horizontal direction and a pressure decrease is noticed. The bubble with a

large width D_B becomes unstable, and the bubble detachment is finally induced.

4. MEASURED PRESSURE AND CONDUCTIVITY SIGNAL

4.1 Comparison of both signals

As presented in the previous section the pressure signal clearly records the complete bubble dynamics in slow bubbling mode, i.e. for small gas flow rate. However Fig. 2 shows that for increasing gas flow rate the pressure signal is not any more representing a reliable, reproducible picture of the bubble behaviour, despite a high recording rate of the measurements.

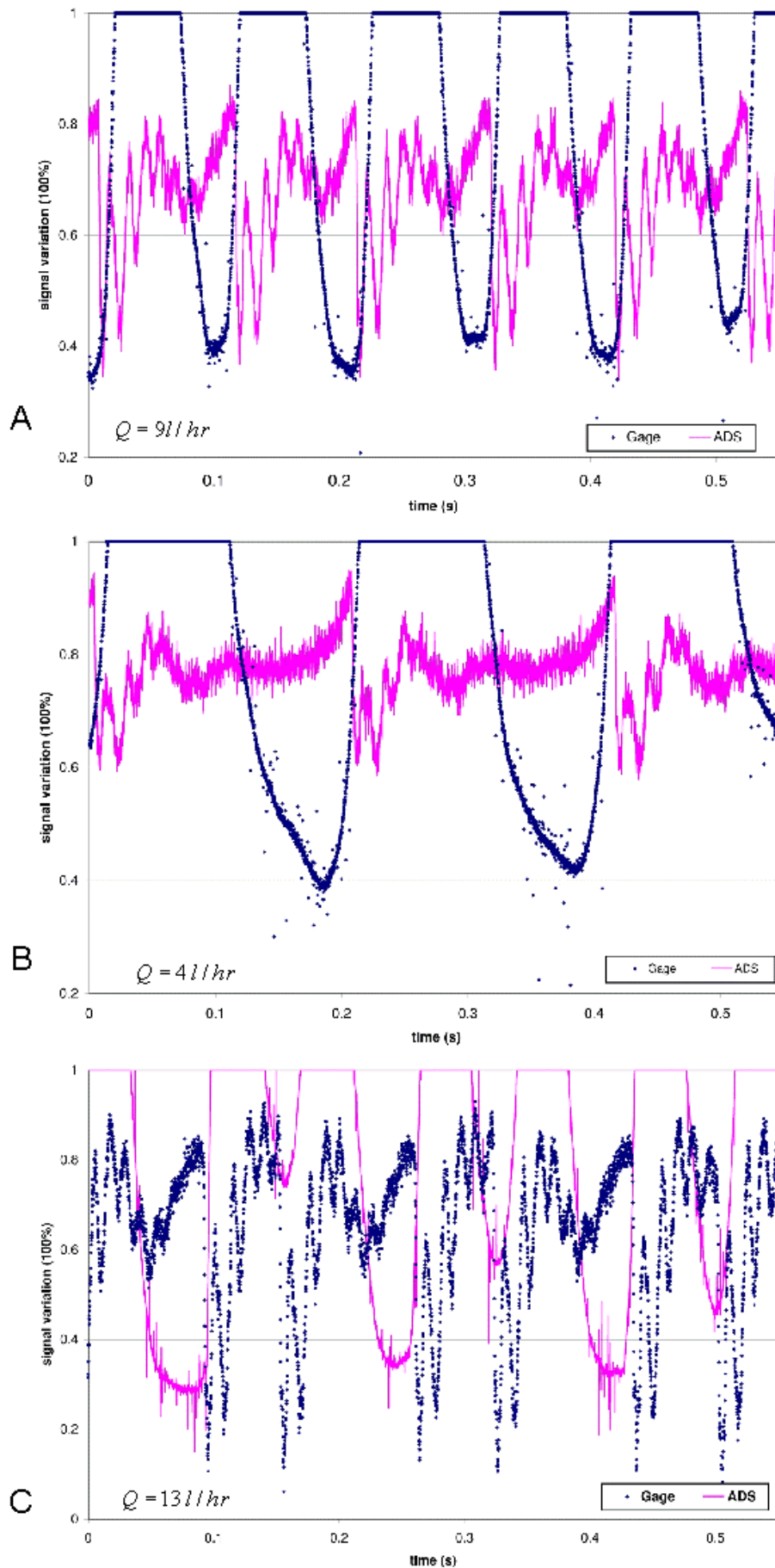


Fig. 4: Pressure and conductivity signal for gas flow rates of 9l/hr (A), 4 l/hr (B) and 13l/hr (C).

At high air flow rate with a high bubble detachment frequency, the so-called fast bubbling mode, the phenomena of necking and detaching or pinching off can not precisely be indicated. Instead the electrical conductivity signal still allows to follow the detachment from the external, electrically isolated tube and detects all pinching off points as represented in Fig. 4.

4.2 Sensitivity of Conductivity Signal on the Gas/Liquid Properties.

Not only the gas flow rate but also the salt concentration of the liquid solution influence the electrical conductivity signal. The impact of both parameters on the recorded conductivity signal has been evaluated and the results are represented in Fig. 5. The sensitivity study yields the following validity range for the electrical conductivity signal: solution concentrations of $0.1\text{g/l} < c < 1\text{g/l}$ and gas flow rates $7\text{l/hr} < Q < 12\text{l/hr}$. Under these operation conditions the conductivity measurements indicated more precisely the bubble detachment or pinching off points than pressure measurements.

5. CONCLUSION

Two methods for checking the status of a dip tube's tip, by pressure recording and by conductivity recording, have been experimentally investigated under slow, normal and fast bubbling mode. Although the pressure signal visualises clearly the dynamic bubble growth with gas/liquid interface oscillations in the slow bubbling mode, the signal can not longer be interpreted unambiguously in the fast bubbling mode. Instead the electrical conductivity signal detects all pinching off points.

Therefore the electrical conductivity signal can be utilised to follow the bubble detachment at dip tubes with an air supply of $7\text{l/hr} < Q < 12\text{l/hr}$ and immersed in aqueous solutions with a concentration of $0.1\text{g/l} < c < 1\text{g/l}$. This alternative method by recording the electrical conductivity will be applied to analyse the pressure signal in fast bubbling mode. The mean

detachment bubble diameter and corresponding detachment frequency, which can be unambiguously determined from the conductivity signal allows to setup a bubble growth model at the tip of a dip tube. This can be utilised to interpret the pressure signal in a reprocessing plant in fast bubbling mode.

6. REFERENCES

- Clanet, C. and Lasheras, J. C., Transition Form Dripping to Jetting, *J. Fluid Mech.*, **383**, pp.307-326, (1999)
- Clift, R. and Grace, J.R. and Weber, M.E., *Bubbles, Drops and Particles*, Acad. Press, (1978)
- Georgescu, S.-C. and Achard, J.-L., Loi de Tate: Analyse Critique et Restrictions, *Proc. XVIeme Congres Français de Mécanique*, pp. 113-120, (2001)
- Platzer, R. and Neuilly, M. and Carrier, M. and Dedaldechamp, P., Mesures de densité et de volume a l'entrée des usines de retraitement, *Proc. ESARDA Symposium*, (1985)
- Rayleigh, Lord, Investigations in Capillarity: The Size of Drops. - The Liberation of Gas from Supersaturated Solutions. - Colliding Jets. - The Tension of Contaminated Water-Surfaces. - A Curious Observation, *Phil. Mag.*, **48**, pp. 321-337, (1899)
- Tate, T., On the Magnitude of a Drop of Liquid Formed under Different Circumstances, *Phil. Mag.*, **27**, pp. 176-180, (1864)
- Taylor, G.I., The Dynamics of Thin Sheets of Fluid. {III}. Disintegration of Fluid Sheets, *Proc. R. Soc. Lond.*, **253, A**, pp. 313-321, (1959)
- Uchikoshi, S. and Watanabe, Y. and Yasu, K. and Matsuda, Y., Fundamental Study for Bubble Formation on Dip-Tube, *Proc. ESARDA Conf.*, pp.1-6, (1996)

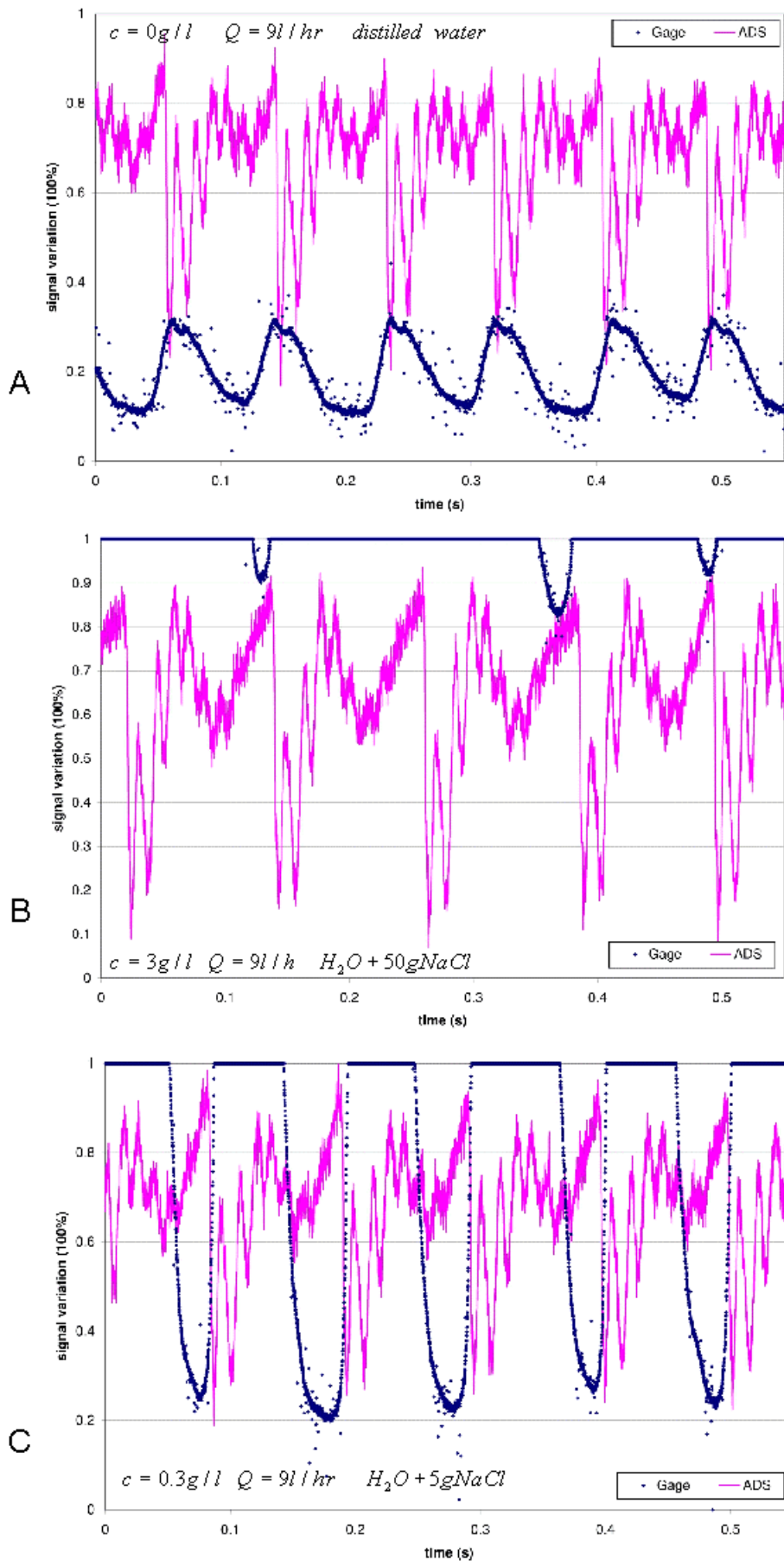


Fig. 5: Influence of the salt concentration on the conductivity signal: 0g/l (A), 0.3g/l(B), 3g/l (C)